Carbohydrate Polymers 115 (2015) 401–407

Contents lists available at ScienceDirect

Carbohydrate Polymers

journal homepage: www.elsevier.com/locate/carbpol

Effects of glycerol on the molecular mobility and hydrogen bond network in starch matrix

Jun Liang [1], Richard D. Ludescher*

Department of Food Science Rutgers, The State University of New Jersey, 88 Lipman Dr., New Brunswick, NJ 08901, United States

ARTICLE INFO

Article history:
Received 3 March 2013
Received in revised form 21 August 2014
Accepted 21 August 2014
Available online 16 September 2014

Keywords:
Starch
Glycerol
Antiplasticization
Molecular mobility
Hydrogen bond network

ABSTRACT

The effects of glycerol on molecular mobility and hydrogen bonding network in an amorphous glassy starch matrix were studied using phosphorescence and IR spectroscopy. Amorphous potato starch films containing varying amounts of glycerol (0, 5, 10, 20 and 30 wt.%) were formulated by rapidly dehydrating aqueous potato starch gel (5%, w/v) with a corresponding content of glycerol; X-ray diffraction data confirm that the films contained negligible content of crystalline starch. Erythrosin B (Ery B) phosphorescence was used to monitor the molecular mobility of these matrices over the temperature range from 0 to 100 °C. Analysis of Ery B emission peak frequency, band width and intensity decay provided information about thermally-activated modes of molecular mobility in the matrix. Dipolar relaxation around the triplet state of Ery B was enhanced by addition of glycerol and the extent of relaxation increased at low and intermediate but decreased at higher temperature. The glycerol content-dependent onset temperature for this transition was 70 °C for pure starch and decreased to 40 °C for a matrix with 30% glycerol. Measurements of the rate of non-radiative decay from the Ery B triplet state indicated that glycerol plasticized the starch matrix above ~10 wt.% while acting as an antiplastizer to increase the matrix molecular mobility at lower content. These matrix properties were related to glycerol-dependent increases in hydrogen bond strength as measured by IR.

1. Introduction

Over the last few years, there has been a renewed interest in biodegradable plastics made from annually renewable, natural polymers (Lawton, 1996). An important renewable raw material is starch. Starch is a versatile food ingredient and is widely used as a texturizer, thickener, gelling agent, adhesive, and moisture-retainer. One of the basic properties of starch is its film-forming ability. Starch consists primarily of branched and linear chains of glucose molecules, namely amylopectin and amylose, respectively. The film-forming ability of starch is principally due to hydrogen bonds between the long-chain, unbranched amylose. Although tensile strengths of starch films are high, they are brittle and exhibit little or no elongation (Lawton & Fanta, 1994). Thus, a plasticizer is always added to increase flexibility. As one of the most commonly used plasticizers, glycerol is compatible with amylose and could interfere with amylose chain packing (Garcia, Martino, & Zaritzky, 1999; Jansson & Thuvander, 2004).

Numerous studies have investigated the physical characteristics of starch-based films and the mechanism underlying film formation (Das et al., 2010; Dufresne & Vignon, 1998; Otey, Westhoff, & Doane, 1987; Lee et al., 2010). The potential applications of starch films are closely related to the film microstructure (Romera, Moraes, Zoldan, Pasa, & Laurindo, 2012), film-forming conditions (Jonhed, Andersson, & Järnström, 2008), and interactions among the components in the starch films (García, Martino, & Zaritzky, 2000). The pure starch amorphous solid could have a high T_g of around 230 °C (Orford, Parker, Ring, & Smith, 1989). Although foods are considered stable in the glass below T_g due to an absence of large-scale molecular motions, and thus the T_g may be a useful index temperature for stability in some amorphous foods, various physical and chemical reactions can still occur in the glassy state, indicating that T_g cannot be considered as a threshold temperature for stability and that molecular mobility below T_g cannot be neglected.

The effects of glycerol on the physical properties of amorphous starch have also been studied. It has been reported that glycerol can exert different effects depending on its concentration. Lourdin, Bizot, and Colonna (1997a) reported that glycerol at a content below 12 wt.% could decrease the ductility of potato starch film;

* Corresponding author. Tel.: +1 8489323516.
E-mail address: ludescher@aesop.rutgers.edu (R.D. Ludescher).
[1] Current affiliation: Institute of Agro-products Processing Science and Technology, CAAS, Beijing 100193, China.

http://dx.doi.org/10.1016/j.carbpol.2014.08.105
0144-8617/

when the amount of glycerol exceeded 12%, however, the ductility increased. Similar antiplasticizing effects of glycerol were also found in the matrixes of trehalose and maltodextrin (Anopchenko, Psurek, VanderHart, Douglas, & Obrzut, 2006; Roussenova, Murith, Alam, & Ubbink, 2010). In most cases, there exists a critical glycerol content that marks the onset of a change in functionality from antiplasticizer to plasticizer. These results, however, were obtained using macroscopic methods like DSC, film stress analysis, and positron annihilation lifetime spectroscopy. Data concerning how glycerol can affect the molecular mobility and interaction forces in the starch and other polymer matrix on the microscopic level are, as far as we know, limited.

Starch films are hydrogen-bonded solids and so the properties of the matrix are modulated by hydrogen bonding interactions among the molecules in the matrix. Wolkers, Oldenhof, Alberda, and Hoekstra (1998) and Wolkers, Oliver, Tablin, and Crowe (2004) established that the OH stretching vibration at ~3300 cm^{-1} increases with the temperature in seven amorphous sugars and ν_{OH}(T) displayed a characteristic change in slope at the sugar T_g's. This increase in ν_{OH} reflects a change from associated hydroxyl to free hydroxyl following the increase of temperature. Recently, we have used FTIR to evaluate the influence of glycerol on the physical state of amorphous solid glucose. We found that addition of glycerol can broaden the distribution of stretching orientations and thus broaden the absorption band from stretching of OH, consistent with the increase in molecular mobility (Liang & Ludescher, 2012).

Here we report studies of the influence of glycerol on molecular mobility in amorphous potato starch obtained from analysis of the phosphorescence from Ery B embedded in the matrix. Glycerol weight content was varied from 0 to 30% by addition of glycerol to the starch solution before film formation. The temperature-dependence of mobility was measured and analyzed at different glycerol contents, generating families of mobility versus temperature curves. Samples in the same conditions were measured by FTIR in the temperature range from 30 to 100 °C. By studying the relation between mobility and hydrogen bond strength and network, we seek to understand how glycerol can modulate the starch matrix mobility as a function of concentration.

2. Materials and methods

2.1. Sample preparation

We prepared amorphous starch films containing varying content of glycerol by using a slightly modified version of our published methods for making sugar/glycerol films (Liang & Ludescher, 2012). Potato starch (Sigma Chemical, St. Louis, MO), 2.5 g, was dissolved in 50 ml deionized water and heated to boiling on a stir plate for at least 10 min to make sure starch was totally denatured. Glycerol (99% GC pure; Sigma Chemical, St. Louis, MO) was added to obtain the final content of 0, 5, 10, 20 or 30% of the dry weight of starch. The glycerol–starch solutions were stirred at room temperature for at least half an hour to make sure the glycerol was totally blended with starch. For the luminescence experiments, starch-glycerol mixtures were prepared from solutions containing erythrosin B at the appropriate concentration. Erythrosin B (Ery B; Sigma Chemical, MO), disodium salt, was dissolved in deionized water to prepare a 10 mM stock solution; an aliquot from this solution was added to the starch solution to obtain a mole ratio of $1:10^4$ for dye/glucose unit in the starch.

The starch solutions were cooled down to room temperature prior to spreading 15 μl on approximately one third of a quartz slide (30 × 13.5 × 0.6 mm, custom made by NSG Precision Cells, Farmingdale, NY). The slides were placed under a gentle warm air stream using an air gun to rapidly (within 5 min) evaporate the moisture.

Slides were soaked in Terg-A-Zyme (Alconox, Inc., NY) soap solution over 24 h to remove surface impurities, then washed with deionized water, and finally rinsed with ethanol and dried with acetone before using.

For the experiments using IR and X-ray, the films were prepared with the same method as that for luminescence except that the sample solutions were spread on ATR plates for the IR experiment or glass slides for the X-ray experiment. The quartz slides, ATR plates and glass slides with film were stored at room temperature against the desiccant Drierite for at least 1 week and kept in an atmosphere of P_2O_5 in order to maintain 0% RH. The desiccant P_2O_5 was refreshed as necessary.

2.2. X-ray diffraction

X-ray diffraction data were taken with a Philips (Model 42273) X-ray diffractometer (Mahwah, NJ), using the following conditions: target, Cu-$k\alpha$ radiation; voltage, 35 kV; current, 20 mA; scanning speed, 2° of 2θ/min; time constant, 1 s. The intensity was measured at a scanning angle (2θ) from 10 to 35°.

2.3. Differential scanning calorimetry

Thermal transitions of starch films were measured with a TA Instruments (model Q200) DSC instrument (Newcastle, DE) in an inert environment by using nitrogen with gas flow rate of 50 ml/min. About 1 mg of each sample was crimp sealed in an aluminum pan. An empty pan was used as a reference. The samples were heated at 10 °C/min and glass transition temperature (T_g) was determined from the midpoint temperature of the change in slope of the heat flow curve.

2.4. Phosphorescence measurements and analysis

All luminescence measurements were conducted on a Cary Eclipse spectrophotometer (Varian Instruments, Walnut Creek, CA) equipped with a temperature controller and multicell holder. All measurements were made at least in triplicate and the temperature was varied from 0 to 100 °C.

A high purity nitrogen stream was routed into the sample compartment and directly into the quartz fluorescence cuvettes that held the slides. The cuvette was capped with a lid having inlet and outlet ports for the gas line, so all experiments were performed at ambient pressure. Each intensity decay was averaged over 50 cycles. For each cycle, data were collected from a single flash with a resolution of 0.04 ms. a 0.05 ms gate, and 10.0 ms total decay time. Phosphorescence and delayed fluorescence emission scans were collected over the range from 540 to 800 nm with an excitation wavelength of 520 nm. The excitation and emission monochromators were both set at 20 nm band pass. Each datum point (collected at 1 nm intervals) was collected from a single flash with 0.2 ms delay and 5 ms gate time.

For lifetime measurements, because intensity decays are distinctly non-exponential, a stretched exponential function was selected to analyze the intensity decays:

$$I(t) = I(0)\exp\left[-\left(\frac{t}{\tau}\right)^{\beta}\right] + \text{constant} \quad (1)$$

where I (0) is the initial intensity, τ is the stretched exponential lifetime, and β is an exponent varying from 0 to 1 that characterizes the lifetime distribution (Pravinata, You, & Ludescher, 2005). The use of stretched exponential model provides an analysis in terms of a continuous distribution of lifetimes, which is appropriated for describing a complex amorphous solid possessing a distribution of

relaxation times for dynamic molecular processes (Richert, 2000; Shirke, Takhistov, & Ludescher, 2005).

The energy of the emission maximum (ν_p) and bandwidth (FWHM, full-width-at-half-maximum) of the emission band were determined by using a log-normal line shape function to fit both delayed fluorescence and phosphorescence emission (Pravinata et al., 2005).

$$I(\nu) = I_0 \quad \exp\left\{-\ln(2)\left(\frac{\ln\left[1+2b\left(\nu-\nu_p\right)\right]/\Delta}{b}\right)^2\right\} \tag{2}$$

where I_0 is the maximum emission intensity, ν_p is the peak frequency (cm^{-1}), Δ is a linewidth parameter, and b is an asymmetry parameter. The bandwidth Γ (FWHM) is calculated according to the following equation:

$$\Gamma = \Delta\left[\frac{\sin\ h(b)}{b}\right] \tag{3}$$

For delayed luminescence spectra collected from 540–750 nm, a sum of log-normal functions for delayed fluorescence ($I_{DF}(\nu)$) and phosphorescence ($I_P(\nu)$) was used to fit the spectra. Each emission band was analyzed for independent fit parameters using a sum of two functions as described in Eq. (2).

The phosphorescence lifetimes were used to calculate the rate constants associated with the various processes that depopulate the triplet state. Our analysis of the delayed emission is similar to the photophysical scheme for Ery B outlined in an earlier study, only using slightly different nomenclature (Duchowicz, Ferrer, & Acuña, 1998). The measured phosphorescence lifetime (τ) is the inverse sum of all possible de-excitation rates for the triplet state T_1.

$$\frac{1}{\tau} = k_P = k_{PR} + k_{TS1} + k_{TS0}. \tag{4}$$

Here, k_{PR} is the rate of radiative decay to the ground state, k_{TS1} is the rate of reverse intersystem crossing to S_1, and k_{TS0} is the rate of intersystem crossing to the singlet manifold followed by vibrational relaxation to S_0; the oxygen quenching term is not included as it is negligible under our experimental conditions. The radiative decay rate has a value of 41 s^{-1} for Ery B (Duchowicz et al., 1998).

Reverse intersystem crossing is a thermally activated process that has an exponential dependence on the energy gap ΔE_{TS} between T_1 and S_1 (Nack & Ludescher, 2006).

$$k_{TS1}(T) = k^o_{TS1} \quad \exp\left(\frac{-\Delta E_{TS}}{RT}\right) \tag{5}$$

The ratio of intensity of delay fluorescence (I_{DF}) to phosphorescence (I_P), where I_{DF} and I_P are determined from analysis of emission spectra using the log-normal function (Eq. (2)), is proportional to the rate of reverse intersystem crossing. A plot of $\ln(I_{DF}/I_P)$ versus $1/T$ thus has a slope of $-\Delta E_{TS}/R$. The singlet-triplet energy gap of Ery B is greatly influenced by the surrounding solvent (matrix) (Lettinga, Zuilhof, & van Zandvoort, 2000). The k^o_{TS1} for Ery B varies from 0.3×10^7 s^{-1} in ethanol (Lettinga et al., 2000) and 6.5×10^7 s^{-1} in water to 111×10^7 s^{-1} in solid polyvinyl alcohol. We estimated the maximum possible value for k^o_{TS1} in starch/glycerol by assuming that $k_{TS1}(T)$ cannot result in values for k_{TS0} decreasing with increasing temperature. This procedure thus estimated the minimum possible values of $k_{TS0}(T)$. The estimated value of k^o_{TS1} was 3×10^7 s^{-1} in this study.

One of the non-radiative decay routes is through intersystem crossing to the ground state S_0. The decay rate is expressed by k_{TS0}, which reflects the rate of collisional quenching of probe due to both internal and external factors (Pravinata et al., 2005). The term k_{TS0} primarily reflects the external environmental factors since the self-collisional quenching among probe molecules can be neglected due to the low concentration and slow diffusion within the extremely viscous amorphous solid. We have used the Ery B probe in numerous studies of amorphous carbohydrate and protein solids and found no evidence of clustering. In particular, as summarized in You and Ludescher (2006): studies of the effect of probe concentration in amorphous sucrose reveal that all measured spectroscopic parameters (emission peak frequency, lifetime, etc.) are identical over the range from 0.5 to 10×10^{-4} probe/sucrose, whereas this study used 1×10^{-4} ratio of probe/glucose monomer; the emission spectra in amorphous starch do not exhibit the characteristic features associated with exciton interactions associated with clustering (spectral broadening splitting of emission band, wavelength shifts) seen in other studies. In this study, the temperature–dependent term k_{TS0} can be calculated from measured lifetimes using Eq. (4).

2.5. Atomic force microscopy (AFM)

Tapping mode AFM images were collected using a NanoScope IIIA Multimode AFM (Veeco Instruments Inc., Santa Barbara, CA) equipped with a silicon-etched RTESP7 cantilever (Veeco Nanoprobe, Camarillo, CA) under ambient conditions. Before tip engagement, the films were check with affiliated microscopy for possible phase separation and the drive frequency of the silicon tip was tuned with the aid of Nanoscope 5.30 software and fixed at 200–250 kHz for further scanning. All of the collected images were smoothed before further analysis.

2.6. Attenuated total reflectance Fourier transform infrared (ATR-FTIR) spectroscopy

The ATR-FTIR spectra were collected by using a Thermal Nicolet Nexus 670 FT-IR spectrometer (Thermo Fisher Scientific Inc., Waltham, MA) equipped with a Smart ARK thermal accessory and analyzed using the associated EZ-OMNIC software. Each spectrum was an average of 102 scans with 4 cm^{-1} resolution in a dry atmosphere of air-dried over P_2O_5 to minimize the interference of moisture in ambient condition. The measurements were conducted at temperatures from 100 down to 30 °C.

3. Results and discussion

During the process of dehydration of the denatured starch solution to form the dried starch films, crystallization can compete with the formation of an amorphous network in amylose. When water is rapidly evaporated, amorphous starch films will be formed with little crystallinity (Talja, 2007). In this study, using X-ray, we confirmed that the starch matrices formed in this way were essentially amorphous (data not included), showing negligible crystallinity.

3.1. Delayed emission spectra

The delayed emission spectra of Ery B in amorphous starch/glycerol films has a long wavelength emission (maximum ~690 nm) due to phosphorescence from the triplet state T_1 and a short wavelength emission (maximum ~555 nm) due to delayed fluorescence from the singlet state S_1 repopulated by thermally activated reverse intersystem crossing from T_1. Delayed emission spectra in starch with variable glycerol content collected over the temperature range from 0 to 100 °C showed a decrease in phosphorescence (I_P) and an increase in delayed fluorescence (I_{DF}) intensity with increasing temperature (data not shown). The intensity ratio was analyzed as $\ln(I_{DF}/I_P)$ versus $1/T$ and the linear slope was used to estimate the energy gap (ΔE_{TS}) separating the excited triplet and singlet states; the energy gap was used to calculate the rate of

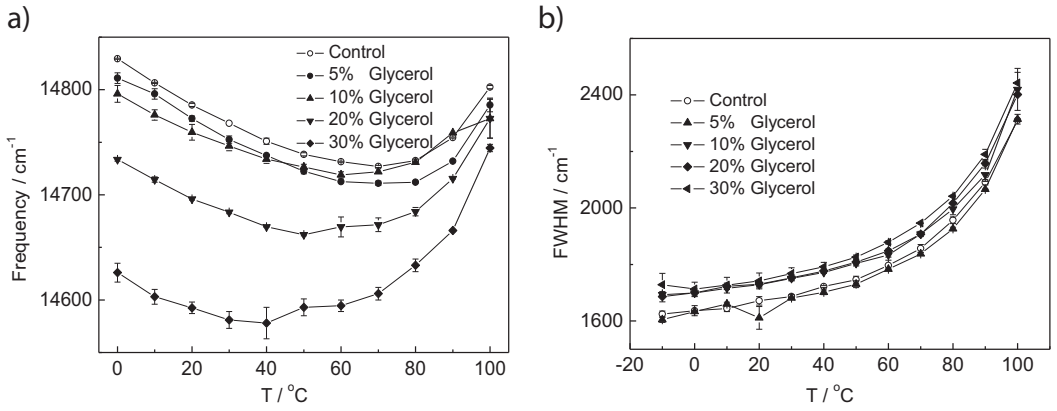

Fig. 1. (A) Peak frequency for phosphorescence emission from Ery B in amorphous starch-based films with varying weight contents of glycerol. (B) Band width (FWHM) for phosphorescence emission from Ery B in amorphous starch-based films with varying weight contents of glycerol.

reverse intersystem crossing, $k_{TS1}(T)$, according to Eq. (5) (see Section 2 for further details). Such plots were linear with $R^2 \geq 0.995$; the slopes from starch samples containing various glycerol contents showed negligible differences (data not shown), indicating that the energy gap, and thus $k_{TS1}(T)$, was not greatly affected by addition of glycerol.

The peak frequency (ν_P) and bandwidth (Γ) for both delayed fluorescence and phosphorescence emission were determined by fitting to a log-normal line shape function (Eqs. (2) and (3)). The parameters of this fitting process are plotted in Fig. 1 for temperatures from 0 to 100 °C. The values of ν_P decreased gradually and approximately linearly at low temperature and increased at high temperature in all samples. The onset temperature for this reversal was ~70 °C in pure starch and decreased with addition of glycerol to ~40 °C for starch with 30 wt.% glycerol. The peak frequency decreased with increasing glycerol content at all temperatures; since glycerol also caused a decrease in the Ery B phosphorescence lifetime (discussed below), this decrease in ν_P indicates that the rate of dipolar relaxation around the excited triplet state increased with glycerol content (Pravinata et al., 2005). Glycerol had a much larger effect on the extent and thus the rate of dipolar relaxation at low temperature than at high temperature.

The increase in ν_P at higher temperature, observed for the first time for this probe in amorphous biomaterials, indicates a temperature-dependent change in the matrix structure around the probe. This structural reorganization increased the energy of the Ery B emission either by decreasing the local matrix polarity and/or hydrogen bonding ability around the probe or by decreasing the extent, and perhaps the rate, of dipolar relaxation during the probe's excited state lifetime. Given that the increase in emission energy also occurred to a comparable albeit lesser extent in pure starch, this structural reorganization was facilitated, but not caused, by glycerol.

The phosphorescence bandwidth reflects the range of energetically distinct matrix environments due to interactions between the matrix molecules and the excited probe (Pravinata et al., 2005). The bandwidth increased gradually and approximately linearly at low temperature and increased dramatically at temperatures above 60 °C in all films (Fig. 1B). The bandwidth was unaffected by addition of 5 wt.% glycerol but increased slightly at higher content of glycerol. Since the increase in bandwidth reflects a corresponding increase in the width of the distribution of energetically distinct matrix environments for the EryB probe, glycerol at 10 wt.% and higher caused a small increase in this distribution over the whole temperature range.

3.2. Emission lifetimes

Glycerol can act both as an antiplasticizer to increase matrix rigidity when present at low content and as a plasticizer to decrease matrix rigidity when present at high content (Lourdin, Coignard, Bizot, & Colonna, 1997b; Lourdin, Ring, & Colonna, 1998). The weight fraction at which glycerol changes from acting as an antiplasticizer to acting as a plasticizer differs based on the physical properties of the matrix. We have identified this transition point for glycerol at ~6 wt.% in amorphous sucrose films using the Ery B phosphorescence probe (You & Ludescher, 2007).

The phosphorescence emission intensity decay transients from Ery B in films of starch/glycerol (under nitrogen) were collected as a function of temperature from 0 to 100 °C. All intensity decay transients were well-fit using a stretched exponential decay model (Eq. (1), Section 2) providing the lifetime τ and stretching exponent β as model fitting parameters; the R^2 was ≥0.995 for all fits. For all matrices, the phosphorescence lifetime decreased monotonically with increasing temperature; the decrease was gradual at low and steeper at high temperature indicating that the various non-radiative decay rates were thermally activated (Fig. 2A). The presence of glycerol affected the Ery B lifetime in a dose- and temperature-dependent manner. At 5 wt.% glycerol the lifetime was unaffected at low temperature (≤40 °C) and increased above that seen in pure starch at higher temperature. At 10 wt.% glycerol the lifetime was decreased below that seen in pure starch at low and intermediate temperature (<80 °C) but unaffected at higher temperature. At 20%, and even more so at 30% glycerol, the lifetime was significantly below that seen in pure starch over the whole temperature range.

The stretching exponent β provides a measure of the width of the distribution of lifetimes that characterizes the excited state decay kinetics of the Ery B probe; β varies between 1 and 0 with lower values indicating a broader distribution. The magnitude of β thus provides a measure of the extent of dynamic heterogeneity in the matrix (Pravinata et al., 2005; Liang & Ludescher, 2012). The value of β exhibited biphasic behavior in all films (Fig. 2B), remaining nearly constant at low to intermediate and decreasing at higher temperature. The magnitude of β and the extent and onset temperature of the decrease varied with glycerol content in a biphasic dose-dependent manner. In pure starch, β was ~0.87 and constant up to ~50 °C and decreased slightly to ~0.8 at 100 °C, indicating that the pure starch matrix became slightly more dynamically heterogeneous at high temperature. The addition of small amounts of glycerol, however, increased β across the entire temperature range; the increase was larger at 5 than at 10 wt.%. At higher glycerol

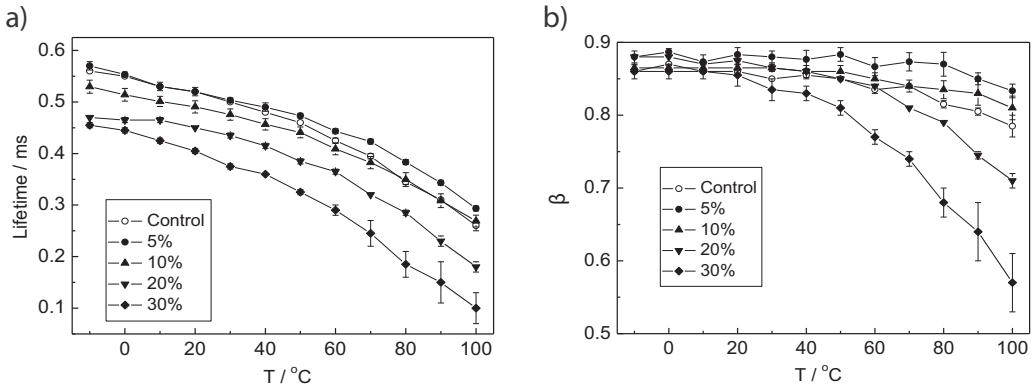

Fig. 2. (A) Temperature-dependence of lifetime obtained from fits to a stretched exponential decay model of the intensity decay of Ery B in amorphous starch-based matrices with varying weight contents of glycerol. (B) Stretching exponent β obtained from fits to a stretched exponential decay model of the intensity decay of Ery B in amorphous starch-based matrices with varying weight contents of glycerol.

content, β decreased in a dose-dependent manner across the entire temperature range. The onset temperature for the decrease in β was also sensitive to the glycerol content, initially increasing from ~50 to ~80 °C at low (5–10 wt.%) and then decreasing to ~40 and ~20 °C at 20 and 30 wt.% glycerol, respectively. The overall matrix dynamic heterogeneity in these starch films was thus slightly decreased and less temperature-dependent at low (≤10 wt.%) and significantly increased and more temperature-dependent at higher glycerol content.

In the absence of oxygen, the lifetime of Ery B reflects values of the rate constants for radiative emission, k_{RP}, reverse intersystem crossing, k_{TS1}, and collisional non-radiative quenching, k_{TS0} (Eq. (4), Section 2). The value of k_{RP} is 41 s^{-1} and constant (Duchowicz et al., 1998; Lettinga et al., 2000). Since the magnitude of k_{TS1} can be estimated from Eq. (5), it is possible to estimate the lower limit of k_{TS0} as a function of temperature. The calculated values for the collisional quenching constant for Ery B in starch/glycerol films as a function of temperature are plotted in Fig. 3 as the value of k_{TS0} in starch/glycerol divided by the value of k_{TS0} in pure starch at the same temperature in order to highlight the effect of glycerol on the matrix mobility. Glycerol decreased the matrix collisional quenching rate, an indicator of local matrix mobility (Pravinata et al., 2005), at low content fractions (<10 wt.%) and increased this rate at high content fractions in a temperature-dependent manner.

Using the same probe, we have previously reported that glycerol acts as an antiplasticizer in sucrose at low weight content (~6%) and low temperature (≤~45 °C) (You & Ludescher, 2007) but not in glucose (Liang & Ludescher, 2012). Our data reported here highlight the importance of molecular structure and specific interactions in mediating the antiplasticization phenomenon in hydrogen bonding carbohydrate matrixes.

3.3. Attenuated total reflectance Fourier transform infrared (ATR-FTIR) spectroscopy

The hydrogen bond is the most important intermolecular interaction determining the properties of the starch matrix. Changes in the hydrogen bond network due to changes in matrix composition or temperature will alter this network and thus modulate matrix structure and mobility. The hydroxyls in solid carbohydrates can be present as either associated hydroxyls, connected with other hydroxyls by hydrogen bonds, or free hydroxyls, not specifically associated with other hydroxyls in hydrogen bonds (Dashnau, Sharp, & Vanderkooi, 2005). While the IR absorbance bands of both types of hydroxyl are distributed above 3000 cm^{-1}, free hydroxyls tend to have higher frequencies (Kondo, 1997). Thus, if associated hydroxyls become free hydroxyls, the IR absorbance band in the hydroxyl region above 3000 cm^{-1} shifts to higher frequency.

The high frequency region due to the OH stretching vibration (3000–3700 cm^{-1}) of starch films with and without glycerol was measured as a function of temperature. The absorbance band above 3000 cm^{-1} shifted to higher frequency for all samples with an increase of temperature, as illustrated for starch with 20 wt.% glycerol (Fig. 4). These data indicate that the increase in temperature shifted the hydrogen bond distribution from associated toward free hydroxyl groups. The decrease in intensity in the region from 3000

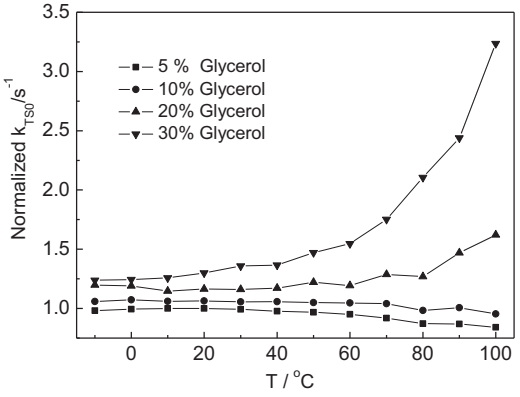

Fig. 3. Rate of non-radiative decay of Ery B triplet state in amorphous starch-based matrices with varying weight content of glycerol. Values are plotted normalized to the value in a pure starch matrix at each temperature. Rate data were calculated from the lifetime data of Fig. 2A.

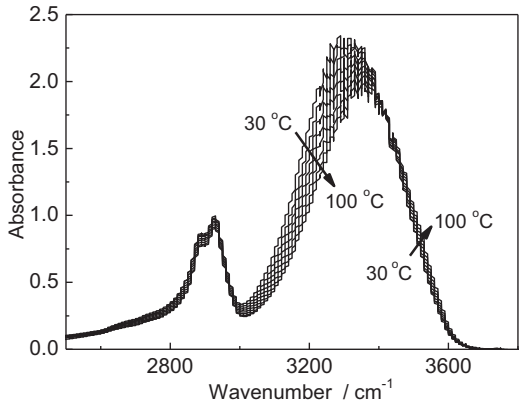

Fig. 4. Temperature-dependence of FTIR spectra of starch matrix with glycerol weight content of 20 wt.%. Orientation of arrow indicates increase in temperature.

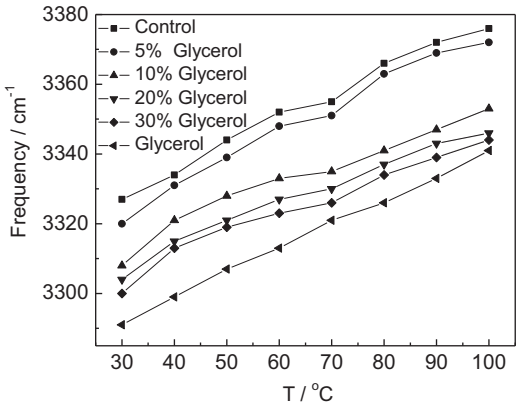

Fig. 5. Temperature-dependence of peak frequency for FTIR spectra above 3000 cm^{-1} in amorphous starch-based matrices with varying weight contents of glycerol.

to 3300 cm^{-1} was more dramatic than the increase in intensity in the region from 3300 to 3600 cm^{-1}. We speculate that this is because the extinction coefficient of associated hydroxyls is larger than that of free hydroxyls. The absorbance over the region from 2700 to 3000 cm^{-1}, attributed to the CH stretch vibration, also decreased with temperature; as the baseline in this region reflects OH absorbance, this decrease is consistent with the effect of temperature on the OH absorbance.

The effect of temperature on the OH absorbance peak frequency of samples containing different content of glycerol is plotted in Fig. 5. The peak frequency, as discussed above, increased with temperature and decreased with glycerol content. The decrease was small at 5 wt.% and considerably larger at 10 wt.% and above. Such a decrease in OH stretching frequency with added glycerol is indicative of a stronger hydrogen bond network.

Investigation of the surface structure of starch-based matrices with and without glycerol using AFM and AFM affiliated microscopy provided no indication of glycerol/starch phase separation in these films (data not shown). It has been seen clearly in previous studies that amylose and amylopectin are arranged in strands that form the network in both starch gels and more compact starch films (Leloup, Colonna, Ring, Roberts, & Wells, 1992). In the rapidly dehydrated films, those strands are further connected in the presence of additives and form into an amorphous solid (Karmas, Buera, & Karel, 1992; Talja, 2007). The polyhydroxyl structure of glycerol can hydrogen bond to polymers like amylose and amylopectin with many polar groups; it thus can strongly interact with the amorphous regions of starch matrices (Soest, de Wit, Tournois, & Vliegenthart, 1994; Kruiskamp, Smits, Soest, & Vliegenthart, 2001). Despite the possibility that contributions from glycerol, which possesses a very low peak OH frequency, cannot be excluded, we interpret the decrease of peak OH frequency in these films as indicating an enhanced hydrogen bond network for the whole matrix.

Amorphous solids are dynamically complex in part because food biomolecules have many modes of molecular mobility, which include all modes of vibrational, rotational, and translational motion that are activated under specified conditions. In rigid solids, many, but certainly not all, of these modes of molecular mobility are effectively damped by molecular interactions that are modulated by matrix composition, temperature, etc. For example, at temperatures below T_g, the local mobility within glasses formed by various glucose oligomers (from glucose to maltoheptaose) was systematically dependent upon the structure and mass of the matrix-forming sugar (Tiwari & Ludescher, 2012). Thermal analysis by DSC indicated that these dry starch samples were glassy under most conditions of this study with T_g values of over 150 °C for samples with 0, 5 and 10 wt.%, 113 °C for 20 wt.%, and 84 °C for 30 wt.% glycerol. Thus, only the highest temperature measurements of the 30 wt.% samples reflect the properties of rubbery films; the continuity of the luminescence and FTIR data curves at high temperature for this sample thus provide no indication of any essential change in molecular behavior of the film through the glass transition.

Plasticizers are typically molecules with low molar mass and consequently greater free volume (Chen et al., 2010). In high concentration, the addition of plasticizers such as glycerol and other small molecules to starch will lower the glass transition temperature (T_g) and make the material properties more rubber-like (de Graaf, Karman, & Janssen, 2003). However, at low concentration in starch, glycerol can act as an antiplasticizer, decreasing elongation at break as well as the moisture and oxygen permeability (Zhang & Han, 2010). These effects may reflect a decrease in the amplitude of localized β-relaxations within the starch matrix (Lourdin et al., 1997a) due to the formation of hydrogen bond based cross-links between small, mobile plasticizer molecules and polymer side chains (Roussenova et al., 2010). The hydrogen bond network is related to free molecular volume and chemical structure of the matrix molecule (Chen et al., 2010) and recent work indicates that molecular mobility is closely related to molecular free volume in carbohydrate/glycerol matrices (Roussenova et al., 2010).

Though hydrogen bonding plays a significant role in modulating molecular mobility, there does not appear to be a rule that can be applied universally. It is expected that stronger intermolecular interactions (that is, more or stronger hydrogen bonds) would decrease mobility; in polymers such as nylons, for example, where β-relaxations can be restricted by hydrogen bonds, the breaking of hydrogen bonds leads to an increase in molecular mobility (Hamada, Iijima, & Gcgregor, 1987). However, in small molecule solid matrices and liquids, where the magnitude of van der Waals potential energy per molecule is comparable with that of hydrogen bonds, the size of the molecule is also a significant factor determining molecular mobility (Naoki & Katahira, 1991). In our previous work, for example, we have found that glycerol does not act as an antiplasticizer of amorphous glucose at low concentration (0.1–0.3 mole ratio) (Liang & Ludescher, 2012), perhaps because the glucose matrix lacks the advanced microstructure found in the potato starch matrix; this microstructure makes the interaction of glycerol with starch more complicated than with glucose.

4. Conclusion

Our data indicate that the mobility of the glassy starch matrix increased with temperature and that this increase was influenced in complex ways by the presence of a low molecular weight glycerol plasticizer and by temperature-dependent decreases and glycerol-dependent increases in hydrogen bond strength. For matrices with low glycerol content (<10 wt.%), the decrease in matrix mobility primarily reflected increases in hydrogen bond strength that enhanced intermolecular interactions, increases that damped the effects of an increase in molecular free volume and thus reduced the expected increase of molecular mobility activated by temperature in the glassy starch matrix. At high glycerol content, on the other hand, the effects of free volume apparently enabled the thermal activation of modes of vibrational and/or translational motion that increased the matrix molecular mobility, effects that overwhelmed any local increase in hydrogen bond strength. The effect of small molecule additives such as glycerol on the properties of amorphous glassy hydrogen bonded solids is clearly complex and structure specific. The work of elucidating how specific molecular interactions modulate the hydrogen bond network and free volume and consequently tune the local and global molecular mobility within the matrix will surely be rewarded with increases in the quality and shelf-life of solid foods and pharmaceuticals.

Acknowledgements

This project was supported by Agriculture and Research Initiative Competitive Grant no. 2009-35503-05226 from the USDA.

References

Anopchenko, A., Psurek, T., VanderHart, D., Douglas, J. F., & Obrzut, J. (2006). Dielectric study of the antiplasticization of trehalose by glycerol. *Physical Review B: Condensed Matter*, *74*, 031501-1–031501-10.

Chen, Z., Huang, W., Fang, P. F., Yu, W., Wang, S. J., Xiong, J., et al. (2010). The hydrogen bond and free volume property of poly(ether-urethane) irradiated by neutron. *Journal of Polymer Science, B: Polymer Physics*, *48*, 381–388.

Das, K., Ray, D., Bandyopadhyay, N. R., Gupta, A., Sengupta, S., Sahoo, S., et al. (2010). Preparation and characterization of cross-linked starch/poly(viny alcohol) green films with low moisture absorption. *Industrial & Engineering Chemistry Research*, *49*, 2176–2185.

Dashnau, J. L., Sharp, K. A., & Vanderkooi, J. M. (2005). Carbohydrate intramolecular hydrogen bonding cooperativity and its effect on water structure. *Journal of Physical Chemistry B*, *109*, 24152–24159.

de Graaf, R. A., Karman, A. P., & Janssen, L. P. B. (2003). Material properties and glass transition temperatures of different thermoplastic starches after extrusion processing. *Starch*, *55*, 80–86.

Duchowicz, R., Ferrer, M. L., & Acuña, A. U. (1998). Kinetic spectroscopy of erythrosin phosphorescence and delayed fluorescence in aqueous solution at room temperature. *Photochemistry and Photobiology*, *68*, 494–501.

Dufresne, A., & Vignon, M. R. (1998). Improvement of starch film performances using cellulose microfibrils. *Macromolecules*, *31*, 2693–2696.

Garcia, M., Martino, M. N., & Zaritzky, N. Z. (1999). Edible starch films and coating characterizations: Scanning electron microscopy, water vapor, and gas permeablilites. *Scanning*, *21*, 348–353.

García, M. A., Martino, M. N., & Zaritzky, N. E. (2000). Lipid addition to improve barrier properties of edible starch-based films and coatings. *Journal of Food Science*, *65*, 941–947.

Hamada, K., Iijima, T., & Gcgregor, R. (1987). Effects of hydrogen bonds on the mobility of spin probes in nylon films. *Polymer Journal*, *19*, 709–717.

Jansson, A., & Thuvander, F. (2004). Influence of thickness on the mechanical properties for starch films. *Carbohydrate Polymer*, *56*, 499–503.

Jonhed, A., Andersson, C., & Järnström, L. (2008). Effects of film forming and hydrophobic properties of starches on surface sized packaging paper. *Packaging Technology Science*, *21*, 123–135.

Karmas, R., Buera, M. P., & Karel, M. (1992). Effect of glass transition on rates of nonenzymatic browning in food systems. *Journal of Agricultural and Food Chemistry*, *40*, 873–879.

Kondo, T. (1997). The assignment of IR absorption bands due to free hydroxyl groups in cellulose. *Cellulose*, *4*, 281–292.

Kruiskamp, P. H., Smits, A. L. M., Soest, J. J. G., & Vliegenthart, J. F. G. (2001). The influence of plasticizer on molecular organisation in dry amylopection measured by differential scanning calorimetry and solid state nuclear magnetic resonance spectroscopy. *Journal of Industrial Microbiology & Biotechnology*, *26*, 90–93.

Lawton, J. W. (1996). Effect of starch type on the properties of starch containing films. *Carbohydrate Polymer*, *29*, 203–208.

Lawton, J. W., & Fanta, G. F. (1994). Glycerol-plasticized films prepared from starch-poly (vinyl alcohol) mixtures: Effect of poly(ethylene-co-acrylic acid). *Carbohydrate Polymer*, *23*, 276–280.

Lee, K. M., Armstrong, P. R., Thomasson, J. A., Sui, R., Casada, M., & Herrman, T. J. (2010). Development and characterization of food-grade tracers for the global grain tracing and recall system. *Journal of Agriculture and Food Chemistry*, *58*, 10945–10957.

Liang, J., & Ludescher, R. D. (2012). Influence of glycerol on the molecular mobility and hydrogen bond network in the glucose-based matrix. *Carbohydrate Research*, *361*, 120–126.

Leloup, V. M., Colonna, P., Ring, S. G., Roberts, K., & Wells, B. (1992). Microstructure of amylose gels. *Carbohydrate Polymer*, *18*, 189–197.

Lettinga, M. P., Zuilhof, H., & van Zandvoort, M. A. M. J. (2000). Phosphorescence and fluorescence characterization of fluorescein derivatives immobilized in various polymer matrices. *Physical Chemistry Chemical Physics*, *2*, 3697–3707.

Lourdin, D., Bizot, H., & Colonna, P. (1997). "Antiplasticization" in starch-glycerol films? *Journal of Applied Polymer Science*, *63*, 1047–1053.

Lourdin, D., Coignard, L., Bizot, H., & Colonna, P. (1997). Influence of equilibrium relative humidity and plasticizer concentration on water content and glass transition of starch materials. *Polymer*, *38*, 5401–5406.

Lourdin, D., Ring, S. G., & Colonna, P. (1998). Study of plasticizer–oligomer and plasticizer–polymer interactions by dielectric analysis: Maltose–glycerol and amylose–glycerol–water systems. *Carbohydrate Research*, *306*, 551–558.

Nack, T. N., & Ludescher, R. D. (2006). Molecular mobility and oxygen permeability in amorphous bovine serum albumin films. *Food Biophysics*, *1*, 151–162.

Naoki, M., & Katahira, S. (1991). Contribution of hydrogen bonds to apparent molecular mobility in supercooled D-sorbitol and some polyols. *Journal of Physical Chemistry*, *95*, 431–437.

Orford, P. D., Parker, R., Ring, S. G., & Smith, A. C. (1989). Effect of water as a diluent on the glass transition behaviour of malto-oligosaccharides, amylose and amylopectin. *International Journal of Biological Macromolecules*, *11*, 91–96.

Otey, F. H., Westhoff, R. W., & Doane, W. M. (1987). Starch-based blown films, 2. *Industrial & Engineering Chemistry Research*, *26*, 1659–1663.

Pravinata, L. C., You, Y. M., & Ludescher, R. D. (2005). Erythrosin B phosphorescence monitors molecular mobility and dynamic site heyerogeneity in amorphous sucrose. *Biophysical Journal*, *88*, 3551–3561.

Richert, R. (2000). Triplet state salvation dynamics: Basics and applications. *Journal of Chemical Physics*, *113*, 8404–8429.

Romera, C. O., Moraes, J. O., Zoldan, V. C., Pasa, A. A., & Laurindo, J. B. (2012). Use of transient and steady-state methods and AFM technique for investigating the water transfer through starch-based films. *Journal of Food Engineering*, *109*, 62–68.

Roussenova, M., Murith, M., Alam, A., & Ubbink, J. (2010). Plasticization, antiplasticization, and molecular packing in amorphous carbohydrate–glycerol matrices. *Biomacromolecules*, *11*, 3237–3247.

Shirke, S., Takhistov, P., & Ludescher, R. D. (2005). Molecular mobility in amorphous maltose and maltitol from phosphorescence of erythrosin B. *Journal of Physical Chemistry B*, *109*, 16119–16126.

Soest, J. J. G., de Wit, D., Tournois, H., & Vliegenthart, J. F. G. (1994). The influence of glycerol on structural changes in waxy maize starch as studied by Fourier transform infrared spectroscopy. *Polymer*, *35*, 4722–4727.

Talja, R. A. (2007). *Preparation and characterization of potato starch films plasticized with polyols*. Helsinki: Department of Food Technology, University of Helsinki (Ph.D. dissertation).

Tiwari, R., & Ludescher, R. D. (2012). Molecular mobility in a homologous series of amorphous glucose oligomers. *Food Chemistry*, *132*, 1814–1821.

Wolkers, W. F., Oldenhof, H., Alberda, M., & Hoekstra, F. A. (1998). A Fourier transform infrared microspectroscopy study of sugar glasses: application to anhydrobiotic higher plant cells. *Biochimica et Biophysica Acta*, *1379*, 83–96.

Wolkers, W. F., Oliver, A. E., Tablin, F., & Crowe, J. H. (2004). A Fourier-transform infrared spectroscopy study of sugar glasses. *Carbohydrate Research*, *339*, 1077–1085.

You, Y. M., & Ludescher, R. D. (2006). Phosphorescence of erythrosin B as a robust probe of molecular mobility in amorphous solid sucrose. *Applied Spectroscopy*, *60*, 813–819.

You, Y. M., & Ludescher, R. D. (2007). The effect of glycerol on molecular mobility in amorphous sucrose detected by phosphorescence of erythrosine B. *Food Biophysics*, *2*, 133–145.

Zhang, Y., & Han, J. H. (2010). Crystallization of high-amylose starch by the addition of plasticizers at low and intermediate concentrations. *Journal of Food Science*, *75*, N8–N16.